Kinetic Study of the Self-Reactions of the $BrCH_2CH_2O_2$ and $BrCH(CH_3)CH(CH_3)O_2$ Radicals between 275 and 373 K

Eric Villenave,* Sandy Moisan, and Robert Lesclaux

Laboratoire de Physico-Chimie Moléculaire, Université Bordeaux I, UMR 5803 CNRS, 33405 Talence Cedex, France

Received: March 29, 2002; In Final Form: September 21, 2002

A conventional flash photolysis technique was used to measure the self-reaction rate constants of the primary $BrCH_2CH_2O_2$ (2-bromoethylperoxy) and secondary $BrCH(CH_3)CH(CH_3)O_2$ (2-bromo-1-methylpropylperoxy) β-brominated peroxy radicals, at temperatures in the range of 275−373 K. The absolute UV absorption spectra of $BrCH_2CH_2O_2$ and $BrCH(CH_3)CH(CH_3)O_2$ were also measured and compared to those obtained previously for these radicals. The temperature dependence of the self-reaction rate constants provided the following Arrhenius expressions: $k(BrCH_2CH_2O_2 + BrCH_2CH_2O_2) = (6.15^{+5.51}_{-2.91}) \times 10^{-14} \exp\{(1247 \pm 203)\ K/T\}$ cm^3 molecule^{-1} s^{-1} and $k(BrCH(CH_3)CH(CH_3)O_2 + BrCH(CH_3)CH(CH_3)O_2) = (7.60^{+22.05}_{-5.65}) \times 10^{-15} \exp\{(1305 \pm 428)\ K/T\}$ cm^3 molecule^{-1} s^{-1}, where the uncertainties represent 95% confidence limits associated with the statistical fitting procedure and include the contribution for the expanded uncertainties in the individual rate constant. These results confirm the enhancement of the peroxy radical self-reaction reactivity upon β-substitution, which is similar for Br, Cl, or OH substituents. Structure−activity relationships are proposed for self-reactions of β-substituted peroxy radicals.

Introduction

Peroxy radicals RO_2 play an important role in atmospheric oxidation processes and in the low-temperature oxidation of hydrocarbons.[1,2] Studies of peroxy radical self-reactions are of interest as a necessary step for studying their reactions with NO_x, HO_2, or other RO_2 compounds. Self-reactions are well-known to present rate constants varying over several orders of magnitude, depending principally on the structure of the radical or on the presence of functional groups.[3−5] It has been shown that substitution of alkylperoxy radicals with hydroxy, carbonyl, or halogen groups, either in the α-position or in the β-position to the peroxy group, significantly increases the self-reaction rate constants.[3,6−10] Although very significant progress has been made in defining structure−reactivity relationships for kinetics of peroxy radical reactions, only a few works have been reported to study the influence of the temperature on the kinetics of substituted peroxy radical reactions.[3] For instance, in the case of the methylperoxy self-reactions, the presence of substituents (F or Cl, whatever their number) results in variations in activation energies of approximately a factor of 2 (with E_a/R values between −400 and −800 K) and variations of a factor of 4 in pre-exponential factors (from 1×10^{-13} to 4×10^{-13} cm^3 molecule^{-1} s^{-1}). When substituents are in the β-position, rate constants of substituted-peroxy self-reactions mainly depend on the class of the radical: for primary and secondary peroxy radicals, β-substitution always yields a negative temperature dependence (with E_a/R values between −700 and −1400 K), whereas, for substituted tertiary radicals, E_a is positive.[3] Hence, the objectives of the present work were to provide further information on the effects of β-substitution on primary and secondary peroxy radicals, by investigating the case of bromine β-substitution at various temperatures in the range of 275−373 K. Kinetics of tertiary β-brominated radical reactions have already been investigated in a previous work by our group.[11] Trends for rate constants and Arrhenius parameters are proposed on the basis of the data available for the self-reactions of various β-substituted peroxy radicals.

A conventional flash photolysis technique was used to determine the rate constant of the following reactions:

$$2BrCH_2CH_2O_2 \rightarrow 2BrCH_2CH_2O + O_2 \quad (1a)$$

$$\rightarrow BrCH_2CH_2OH + BrCH_2CHO + O_2 \quad (1b)$$

$$2BrCH(CH_3)CH(CH_3)O_2 \rightarrow 2BrCH(CH_3)CH(CH_3)O + O_2 \quad (2a)$$

$$\rightarrow BrCH(CH_3)CH(CH_3)OH + BrCH(CH_3)C(O)CH_3 + O_2 \quad (2b)$$

Experimental Section

Kinetic studies were performed at atmospheric pressure, using the conventional flash photolysis technique, coupled with UV absorption spectrometry as real-time monitoring of radical concentrations. This technique has already been described in detail[12] and is addressed only briefly here.

The setup consisted of a 70-cm-long Pyrex reaction cell, fitted with a water-filled thermostat jacket. Flashes were generated by discharging two capacitors through external argon flash lamps. The UV analysis beam from a deuterium lamp was directed along the length of the cell and focused onto the slit of a monochromator. The light intensity at the selected wavelength ($\lambda = 200-300$ nm) was monitored by a photomultiplier tube, and the signal was stored in a digital oscilloscope and transferred to a microcomputer for signal averaging and further data analysis.

* To whom correspondence should be addressed. E-mail address: e.villenave@lpcm.u-bordeaux1.fr.

10.1021/jp0258558 CCC: $25.00
Published on Web 03/12/2003

Brominated peroxy radicals $BrCH_2CH_2O_2$ (2-bromoethylperoxy) and $BrCH(CH_3)CH(CH_3)O_2$ (2-bromo-1-methylpropylperoxy) were generated using the UV−visible photolysis of molecular bromine (Br_2), producing Br atoms that added to the double bond of either ethene (C_2H_4) or (*E*)-but-2-ene (C_4H_8), respectively, in the presence of oxygen and nitrogen:

$$Br_2 + h\nu\ (\lambda > 280\ nm) \rightarrow 2Br \qquad (3)$$

$$Br + CH_2{=}CH_2 + M \rightleftharpoons BrCH_2CH_2 + M \qquad (4,-4)$$

where $k_4(298\ K) = 1.23 \times 10^{-13}$ cm^3 molecule^{-1} s^{-1} in 700 Torr of air,[13] or

$$Br + (CH_3)CH{=}CH(CH_3) + M \rightarrow BrCH(CH_3)CH(CH_3) + M \qquad (5)$$

where $k_5(298\ K) = 8.5 \times 10^{-12}$ cm^3 molecule^{-1} s^{-1} in 750 Torr of molecular nitrogen (N_2),[14,15]

$$BrCH_2CH_2 + O_2 + M \rightarrow BrCH_2CH_2O_2 + M \qquad (6)$$

where k_6 was estimated to be similar to $k(C_2H_4Cl + O_2)$ (1×10^{-11} cm^3 molecule^{-1} s^{-1}) at 298 K,[16] or

$$BrCH(CH_3)CH(CH_3) + O_2 + M \rightarrow BrCH(CH_3)CH(CH_3)O_2 + M \qquad (7)$$

where k_7 was estimated to be larger than $k(s\text{-}C_4H_9 + O_2)$ (1.67×10^{-11} cm^3 molecule^{-1} s^{-1}) at 298 K (in 4 Torr of helium).[17]

The concentration of Br_2 was measured by its absorption at 415 nm ($\sigma = 6.45 \times 10^{-19}$ cm^2 molecule^{-1})[18] and maintained in the concentration range of $1 \times 10^{15}-5 \times 10^{15}$ molecules cm^{-3}. The photolysis yield of Br_2 in our system was calibrated against the acetylperoxy radical absorption formed by replacing ethene (or (*E*)-but-2-ene) by acetaldehyde (which reacts efficiently with Br atoms) before and after each set of experiments, keeping all other experimental conditions identical. Absorption cross sections of $CH_3C(O)O_2$ are well established: $\sigma(207\ nm) = 6.75 \times 10^{-18}$ cm^2 molecule^{-1} and $\sigma(250\ nm) = 3.22 \times 10^{-18}$ cm^2 molecule^{-1}.[2] Under the experimental conditions, initial Br atom concentrations were usually in the range of $2 \times 10^{13}-1 \times 10^{14}$ molecules cm^{-3}.

Concentrations of ethene (and (*E*)-but-2-ene) were chosen such that the conversion of Br atoms to radicals was almost instantaneous, compared to the time scale of the reactions of interest, and dominated all other possible loss processes of Br atoms, in particular, reaction 8:

$$Br + BrCH_2CH_2O_2\ (\text{or } BrCH(CH_3)CH(CH_3)O_2) + M \rightarrow BrCH_2CH_2OOBr\ (\text{or } BrCH(CH_3)CH(CH_3)OOBr) + M \qquad (8)$$

where k_8 was estimated to be similar to $k(C_2H_5O_2 + Br)$ ($\sim 1 \times 10^{-10}$ cm^3 molecule^{-1} s^{-1}) at 298 K and in 1 atm of air.[19]

Concentrations of ethene were typically set in the range of $1 \times 10^{17}-4 \times 10^{18}$ molecule cm^{-3}, and those of (*E*)-but-2-ene were always in the range of $3.5 \times 10^{16}-1 \times 10^{17}$ molecule cm^{-3}. The oxygen partial pressure was varied in the range of 10−730 Torr; however, most experiments were performed under a large excess of molecular oxygen (O_2), to scavenge $BrCH_2CH_2$ radicals rapidly and avoid reaction −4 ($k_{-4}(298\ K) = 1.16 \times 10^6$ s^{-1} in air).[20]

In experiments where the oxygen concentration was varied, nitrogen was used as the diluent gas. The total flow rate in the cell was sufficiently high to ensure that the reaction mixture was completely replenished between each flash, thus preventing complications arising from the reaction products.

Oxygen, nitrogen (AGA Gaz Spéciaux, >99.995%), acetaldehyde (Aldrich, 99%), (*E*)-but-2-ene (Aldrich, >99%), ethene (AGA Gas Spéciaux, 99.8%), bromine (Aldrich, 99.5%), 2-bromoethanol (Aldrich, 95%), and 3-bromo-2-butanone (Lancaster, >97%) were all used without further purification. Liquid compounds (bromine and acetaldehyde) were introduced into the gas mixture by passing a slow flow of nitrogen (or oxygen) through a bubbler cooled in a water−ice bath.

Experimental decay traces (absorbance versus time) were analyzed by numerical integration of a set of differential equations that took into account the complete reaction mechanisms. Resulting simulations were fitted by adjusting selected parameters (i.e., self-reaction rate constants), using nonlinear least-squares fitting.

Results

The kinetic studies of the self-reactions of the $BrCH_2CH_2O_2$ and $BrCH(CH_3)CH(CH_3)O_2$ radicals are reported below. The self-reaction of the 2-bromoethylperoxy radical ($BrCH_2CH_2O_2$) has been selected as a typical case for a detailed presentation of the results. The results for the 2-bromo-1-methylpropylperoxy radical ($BrCH(CH_3)CH(CH_3)O_2$) are reported only briefly, because experiments and data analyses were conducted in a similar way. Therefore, only the particular features specific to this study are noted.

$BrCH_2CH_2O_2$ and $BrCH(CH_3)CH(CH_3)O_2$ Ultraviolet Absorption Spectra. Absolute UV absorption cross sections were required to quantify the radical concentrations of interest in the present work. The UV spectra were obtained by measuring the initial absorption of the decay traces at different wavelengths in the range of 210−290 nm. The presence of a short postflash dead time meant that the decay traces had to be extrapolated to time zero by modeling the decay profile, using the complete reaction mechanisms, as described in the next section. Absolute cross-section values were obtained by calibrating the photolysis yield of Br_2, from which the initial radical concentrations were deduced, as detailed previously.

Spectra of $BrCH_2CH_2O_2$ and $BrCH(CH_3)CH(CH_3)O_2$ radicals are respectively presented in Figures 1 and 2, and the corresponding cross sections are given in Table 1. The UV spectra resemble those of most alkyl peroxy radicals, appearing as a broad band in the range of 200−300 nm, without any vibrational structure and with maxima at 240 nm ($\sigma(BrCH_2CH_2O_2) = (4.77 \pm 0.09) \times 10^{-18}$ cm^2 molecule^{-1} and $\sigma(BrCH(CH_3)CH(CH_3)O_2) = (4.27 \pm 0.16) \times 10^{-18}$ cm^2 molecule^{-1}).

Also shown in Figures 1 and 2 are the spectra measured previously by Crowley and Moortgat[10] for the same radicals, using the molecular modulation technique. Although the shapes of the spectra are similar in both studies, note the discrepancy in the absolute cross-section values at short wavelengths. Cross sections reported by Crowley and Moortgat[10] are 5%−15% lower for $BrCH_2CH_2O_2$ and are quasi-identical for $BrCH(CH_3)CH(CH_3)O_2$ to those determined in this work in the range of 250−290 nm. However, the discrepancies increase at <240 nm, up to 70% at 210 nm. In the molecular modulation experiments, the absolute spectra were calibrated by scaling the UV cross sections to the values obtained at 270 nm for both radicals. Reported spectra were obtained using a deconvolution procedure to take into account the absorption of HO_2 radicals, which absorb significantly at <240 nm and are expected to be produced in the secondary chemistry following the RO_2 self-reaction. This deconvolution procedure, which was performed without con-

TABLE 1: UV Absorption Cross Sections for $BrCH_2CH_2O_2$, $BrCH(CH_3)CH(CH_3)O_2$, $BrCH_2CH_2OH$, and $BrCH(CH_3)C(O)CH_3$ at 298 K

wavelength (nm)	$\sigma(BrCH_2CH_2O_2)^{a,b}$	$\sigma(BrCH(CH_3)CH(CH_3)O_2)^{a,b}$	$\sigma(BrCH_2CH_2OH)^{a,c}$	$\sigma(BrCH(CH_3)C(O)CH_3)^{a,c}$
210	3.05 ± 0.19	2.87 ± 0.17	0.41	0.81
220	3.77 ± 0.07	3.31 ± 0.20	0.23	0.69
230	4.48 ± 0.17	3.98 ± 0.17	0.08	0.44
240	4.77 ± 0.09	4.27 ± 0.16		0.27
250	4.55 ± 0.17	4.22 ± 0.33		0.17
260	3.62 ± 0.11	3.70 ± 0.10		0.14
270	2.29 ± 0.30	2.88 ± 0.19		0.17
280	1.36 ± 0.15	1.66 ± 0.03		0.22
290	0.68 ± 0.04	0.90 ± 0.03		0.27

[a] Given in units of 10^{-18} cm^2 molecule^{-1}. [b] Uncertainties are the 95% confidence level components due to random effects only. [c] Uncertainties are ~15%.

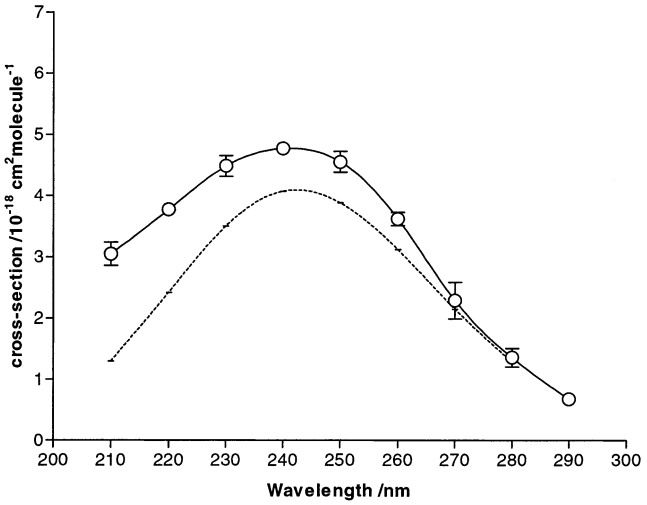

Figure 1. UV absorption spectrum measured in this work (circles) for the $BrCH_2CH_2O_2$ radical, compared to that previously reported by Crowley and Moortgat[10] (dotted line) using the molecular modulation technique.

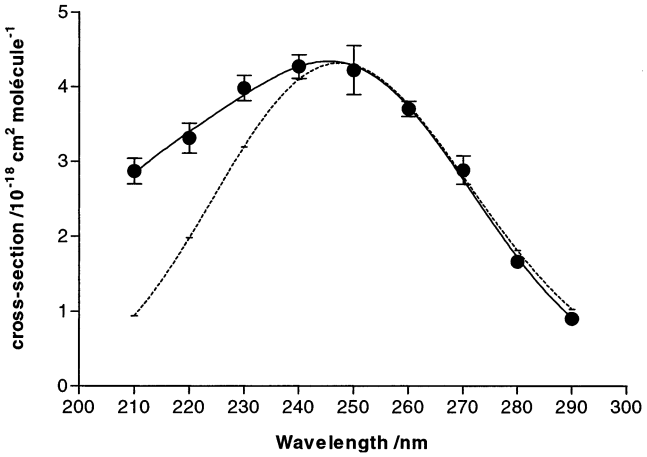

Figure 2. UV absorption spectrum of $BrCH(CH_3)CH(CH_3)O_2$ determined in this work (circles). Dotted line represents that previously reported by Crowley and Moortgat[10] using the molecular modulation technique.

sidering the entire complete mechanism (in particular, the brominated products formed by the peroxy self-reaction), may explain the observed discrepancies at short wavelengths. At longer wavelengths, the differences observed between the two studies are within the uncertainties.

Kinetics of the $BrCH_2CH_2O_2$ Self-Reaction. The kinetic measurements of k_1 were performed at temperatures in the range of 275−373 K, at monitoring wavelengths that were systematically varied over a range of 210−290 nm, and decay traces were recorded over various time scales. Typical experimental traces and their best-fit simulations are presented in Figure 3. By analogy with previous studies of alkylperoxy radical self-reactions, the reaction mechanism for the $BrCH_2CH_2O_2$ self-reaction is as follows:

$$BrCH_2CH_2O_2 + BrCH_2CH_2O_2 \rightarrow 2BrCH_2CH_2O + O_2 \quad (1a)$$

$$\rightarrow BrCH_2CH_2OH + BrCH_2CHO + O_2 \quad (1b)$$

$$BrCH_2CH_2O + O_2 \rightarrow HO_2 + BrCH_2CHO \quad (9)$$

where k_9 was estimated to be similar to $k(CH_3CH_2O + O_2)$ (1.0×10^{-14} cm^3 molecule^{-1} s^{-1}) at 298 K.[21]

$$BrCH_2CH_2O_2 + HO_2 \rightarrow \text{products} \quad (10)$$

where k_{10} was estimated to be similar to $k(CH_3CH_2O_2 + HO_2)$ (7.8×10^{-12} cm^3 molecule^{-1} s^{-1}) at 298 K.[2]

$$HO_2 + HO_2 \rightarrow H_2O_2 + O_2 \quad (11)$$

with $k_{11} = 3.0 \times 10^{-12}$ cm^3 molecule^{-1} s^{-1} at 298 K and in 1 atm of air.[22]

This reaction mechanism is consistent with Fourier transform infrared product studies of the Br-atom-initiated oxidation of ethene,[14,23] which showed that 2-bromoethanol ($BrCH_2CH_2OH$), bromoacetaldehyde ($BrCH_2CHO$), and 2-bromohydroethylperoxide ($BrCH_2CH_2OOH$) are the major reaction products. The branching ratio $\alpha = k_{1a}/k_1$ for the nonterminating channel of reaction 1 was taken to be equal to 0.57.[23] This value is confirmed by the present study, because experimental traces could never be satisfactorily simulated using α values of <0.4 or >0.7. It was assumed that the $BrCH_2CH_2O$ radicals formed via reaction 1a only react with O_2 (under high oxygen concentration) to form HO_2 in the temperature range of interest, because no change was observed in the shape of experimental traces when the temperature was varied.

As shown in Figure 3, the shape of experimental decays depends on the analysis wavelength. At $\lambda > 240$ nm, traces display essentially simple second-order kinetics. At λ values between 210 and 230 nm, the distortion of the decays was characteristic of the formation of significant quantities of HO_2 through reaction 9. In addition, a non-negligible residual absorption was observed at $\lambda < 240$ nm and was attributed mainly to the formation of $BrCH_2CH_2OH$ and $BrCH_2CHO$, in agreement with the end-product studies.[10,14,23] Therefore, UV absorption cross sections of $BrCH_2CH_2OH$ and $BrCH(CH_3)C(O)CH_3$ (which are supposed to be similar to those of $BrCH_2CHO$, which is commercially unavailable) were measured in the range of 210−290 nm using a Hewlett-Packard model 8452A spectrophotometer. They are reported in Table 1. By

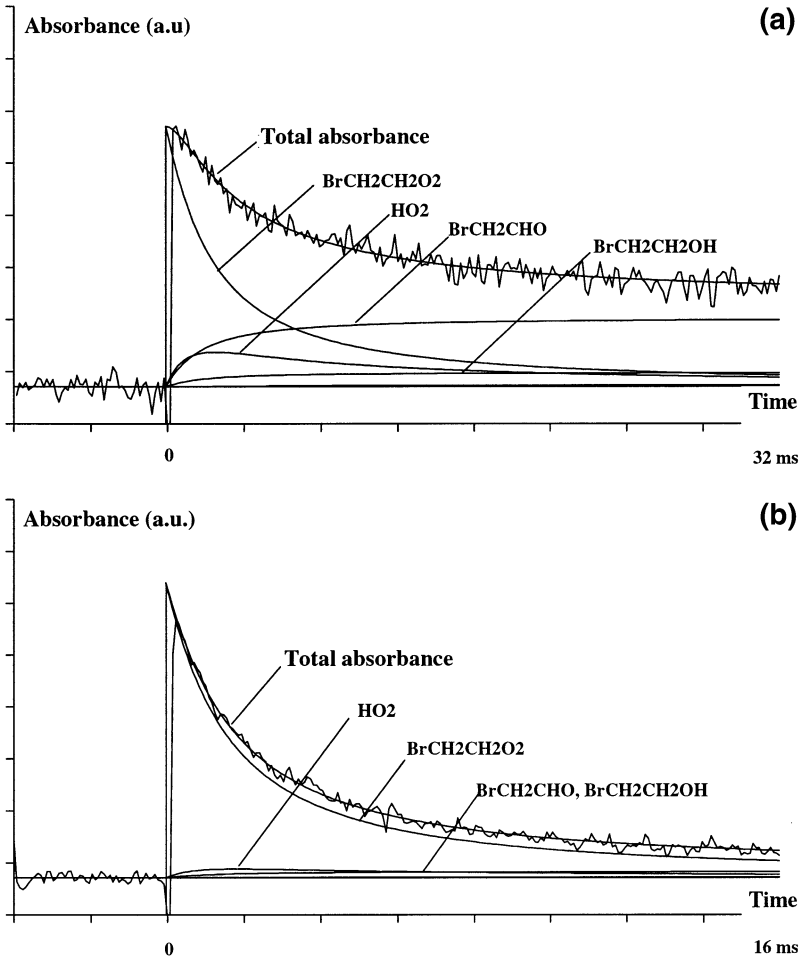

Figure 3. Typical experimental traces recorded at (a) 210 and (b) 240 nm and best-fit simulations for the determination of $k_1(BrCH_2CH_2O_2 + BrCH_2CH_2O_2)$ at 298 K.

TABLE 2: Experimental Values of the Rate Constant for the $BrCH_2CH_2O_2$ Self-Reaction

temp (K)	k_1[a] ($\times 10^{-12}$ cm^3 molecule^{-1} s^{-1})	number of determinations
275	5.51 ± 0.26	12
298	4.49 ± 0.22	14
318	3.00 ± 0.11	7
348	2.11 ± 0.23	6
371	1.80 ± 0.04	8

[a] Errors are the 95% confidence level components due to random effects only.

introducing $BrCH_2CH_2OH$ and $BrCH(CH_3)C(O)CH_3$ cross sections into our model, the residual absorption was fairly well reproduced in the simulations, and the measured rate constants did not vary with the analysis wavelength, which allowed us to validate the mechanism presented earlier.

The dependence of the formation rate of the 2-bromoethylperoxy radical ($BrCH_2CH_2O_2$) on oxygen concentration was investigated at two different analysis wavelengths (210 and 250 nm), by decreasing the oxygen partial pressure regularly from 700 Torr to 10 Torr. If no significant change in the shape of experimental traces was noted at 250 nm, the rates of decay traces obtained at 210 nm were clearly slower for low oxygen concentrations (<150 Torr) than those recorded in 700 Torr of O_2 at the same wavelength. These observations are consistent with those of Barnes et al.,[14] who indicated that the apparent rate constant for the reaction of bromine with C_2H_4 increases as the oxygen partial pressure increases, suggesting the existence of an equilibrium between bromine, ethene (C_2H_4), and $BrCH_2CH_2$. Thus, to avoid such complications, kinetic experiments were always performed under high oxygen concentration (700 Torr).

The results of our experiments on the $BrCH_2CH_2O_2$ self-reaction are summarized in Table 2. A weighted least-squares fit of all the data yields the following Arrhenius expression for k_1 in the temperature range of 275−371 K:

$$k_1 = (6.15^{+5.51}_{-2.91}) \times 10^{-14} \times \exp\{(1247 \pm 203)\ \mathrm{K}/T\}$$
$$\mathrm{cm^3\ molecule^{-1}\ s^{-1}}$$

The corresponding Arrhenius plot is shown in Figure 4. The quoted uncertainties represent 95% confidence limits associated with the statistical fitting procedure and include the contribution for the expanded uncertainties in the individual rate constant.

To quantify the sensitivity of the rate constant k_1 toward the parameters used for analysis, a systematic analysis of error propagation was performed, as described previously.[12] It appears that the rate constant k_1 is mainly sensitive to the variations of $\sigma(BrCH_2CH_2O_2)$, to the branching ratio α, and to the rate constant k_{10} for the $(BrCH_2CH_2O_2 + HO_2)$ reaction. This is particularly true when k_1 is extracted from experimental traces recorded at short wavelengths (λ < 240 nm), where the absorptions of HO_2, $BrCH_2CHO$, and $BrCH_2CH_2OH$ directly influence the decay shapes. Thus, most measurements were performed at wavelengths of >240 nm, where residual absorptions are negligible and the signal-to-noise ratio was its maximum value. Measurements performed at shorter wavelengths allowed us to validate the chemical mechanism. Allowing for errors of ~20% in $\sigma(BrCH_2CH_2O_2)$ resulted in a

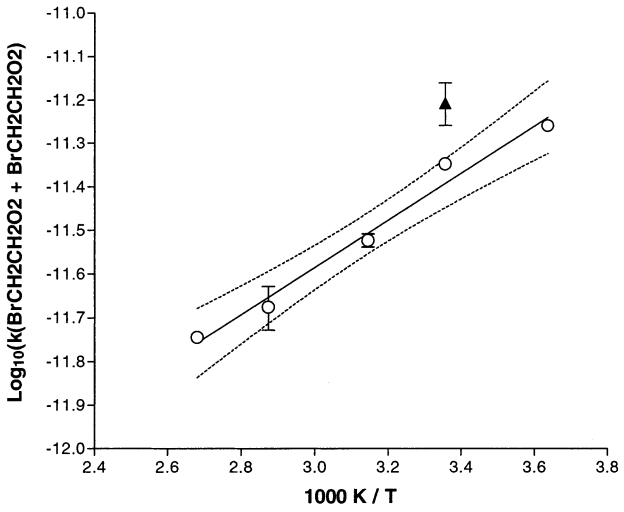

Figure 4. Arrhenius plot for the self-reaction of $BrCH_2CH_2O_2$ (circles). The room-temperature measurement of the overall rate constant k_{1obs}, by Crowley and Moortgat,[10] is represented by the triangle. The quoted uncertainties represent 95% confidence limits associated with the statistical fitting procedure and include the contribution for the expanded uncertainties in the individual rate constant.

variation of 18% in k_1. A variation of 30% in α results in a variation of only 5% at 250 nm but a variation of 27% at 210 nm. Reasonably varying the value of k_{10} by a factor of 2 (from 5×10^{-12} to 1×10^{-11} cm^3 molecule^{-1} s^{-1}) results in a change in k_1 of 6% at 250 nm and 21% at 210 nm. The sensitivity of the fit to the variations of $\sigma(HO_2)$, $\sigma(BrCH_2CHO)$, and $\sigma(BrCH_2CH_2OH)$ was negligible at 250 nm. However, variations of 10% in $\sigma(HO_2)$ and 15% in $\sigma(BrCH_2CHO)$ and $\sigma(BrCH_2CH_2OH)$ respectively result in variations of 15%, 30%, and 10% in the self-reaction rate constant k_1 at 210 nm. All the above-described uncertainties are combined with the statistical errors in an overall uncertainty of ∼30% in k_1.

Kinetics of the $BrCH(CH_3)CH(CH_3)O_2$ Self-Reaction. The self-reaction of the 2-bromo-1-methylpropylperoxy radical,

$$2BrCH(CH_3)CH(CH_3)O_2 \rightarrow 2BrCH(CH_3)CH(CH_3)O + O_2 \quad (2a)$$

$$\rightarrow BrCH(CH_3)CH(CH_3)OH + BrCH(CH_3)C(O)CH_3 + O_2 \quad (2b)$$

was investigated at different temperatures (275−371 K), different wavelengths (210−290 nm), and various time scales (40−200 ms). A typical decay recorded at 250 nm is shown in Figure 5. No data for product yields of the $BrCH(CH_3)CH(CH_3)O_2$ self-reaction were available; thus, the reaction mechanism used in the simulations was similar to that of the $BrCH_2CH_2O_2$ radical self-reaction. All experiments were performed under high oxygen partial pressure (730 Torr), to prevent further complications resulting, on one hand, from a potential equilibrium between Br atoms, C_4H_8, and $BrCH(CH_3)CH(CH_3)$ (as discussed previously for C_2H_4), and, on the other hand, from the possible decomposition of the alkoxy radical $BrCH(CH_3)CH(CH_3)O$ formed via reaction 2a.

$$BrCH(CH_3)CH(CH_3)O + O_2 \rightarrow HO_2 + BrCH(CH_3)C(O)CH_3 \quad (12)$$

Note that the unsubstituted 2-butoxy radical is mainly reacting with O_2 (>90% in 730 Torr of O_2) rather than decomposing (<10%).[24] Decomposition of the $BrCH(CH_3)CH(CH_3)O$ radical would lead to the formation of a new peroxy radical, according to reactions 13 and 14:

$$BrCH(CH_3)CH(CH_3)O + M \rightarrow BrCH(CH_3) + CH_3CHO + M \quad (13)$$

$$BrCH(CH_3) + O_2 + M \rightarrow BrCH(CH_3)O_2 + M \quad (14)$$

No information on both the kinetics and the product yield of $BrCH(CH_3)O_2$ reactions was available; therefore, we proceeded again by analogy to propose a kinetic model that accounts, at best, for the experimental observations. The $BrCH(CH_3)O_2$ radical is the α-brominated analogue of the ethylperoxy radical $C_2H_5O_2$, which presents a well-known self-reaction rate constant, i.e., $k = 6.8 \times 10^{-14}$ cm^3 molecule^{-1} s^{-1} at 298 K.[22] As a primary brominated peroxy radical, we can expect that $BrCH(CH_3)O_2$ presents a higher reactivity than the nonsubstituted ethylperoxy radical.[7] However, the enhancement of the reactivity observed upon β-substitution appears to be less important for α-substituted radicals (see discussion); thus, $BrCH(CH_3)O_2$ should be less reactive than the primary β-brominated $BrCH_2CH_2O_2$ radical studied in this work. Therefore, we have estimated that the rate constant for the $BrCH(CH_3)O_2$ self-reaction was intermediate between those of the $C_2H_5O_2$ and $BrCH_2CH_2O_2$ radicals and set its value at $\sim 2 \times 10^{-13}$ cm^3 molecule^{-1} s^{-1} in simulations. By considering 100% of $BrCH(CH_3)CH(CH_3)O$ decomposition and introducing the $BrCH(CH_3)O_2$ radical chemistry in the simulations, the value of the rate constant k_2 did not vary by >35%. Therefore, considering

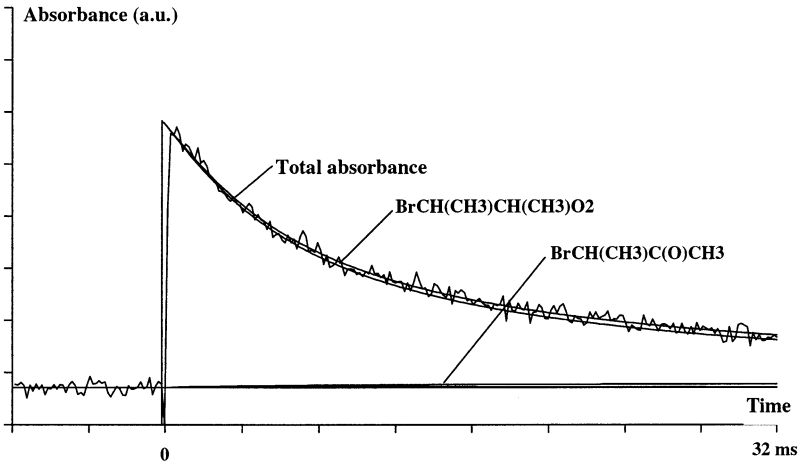

Figure 5. Typical decay trace obtained at 250 nm for the $BrCH(CH_3)CH(CH_3)O_2$ self-reaction at $T = 293$ K.

TABLE 3: Experimental Values of the Rate Constant for the $BrCH(CH_3)CH(CH_3)O_2$ Self-Reaction

temp (K)	k_2[a] ($\times 10^{-13}$ cm^3 molecule^{-1} s^{-1})	number of determinations
275	8.0 ± 0.3	6
293	6.4 ± 0.4	15
318	5.6 ± 0.5	6
343	3.7 ± 0.5	6
371	2.2 ± 0.3	7

[a] Errors are the 95% confidence level components due to random effects only.

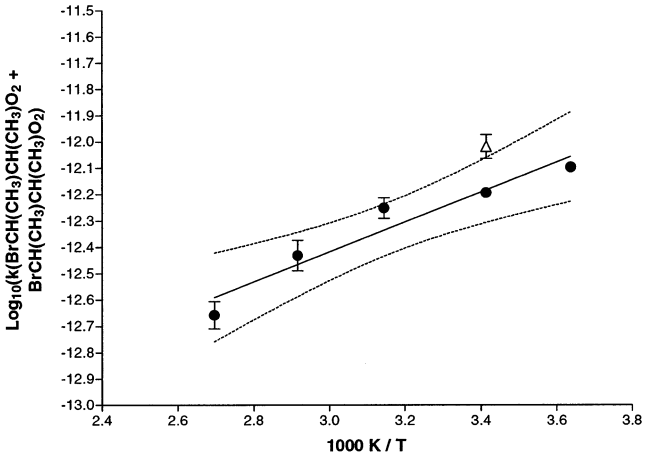

Figure 6. Arrhenius plot for the self-reaction of $BrCH(CH_3)CH(CH_3)O_2$ (circles). The room-temperature measurement of the overall rate constant k_{2obs}, by Crowley and Moortgat,[10] is represented by the triangle. The quoted uncertainties represent 95% confidence limits associated with the statistical fitting procedure and include the contribution for the expanded uncertainties in the individual rate constant.

this additional uncertainty and the recent work of Zabel's group on the unsubstituted 2-butoxy radical,[24] it was finally decided to simplify the mechanism and simulate all experimental traces, accounting only for the reaction of $BrCH(CH_3)CH(CH_3)O$ with O_2, neglecting its decomposition and the $BrCH(CH_3)O_2$ formation under our experimental conditions. The effect of this final assumption is included in the total uncertainties of the rate constant.

At shorter wavelengths, slower experimental decays were observed and interpreted by the presence of HO_2 formed by reaction 12. As in the case of $BrCH_2CH_2O_2$, the residual absorption observed at long time scales and short wavelengths for the $BrCH(CH_3)CH(CH_3)O_2$ self-reaction was attributed to the formation of the corresponding ketone ($BrCH(CH_3)C(O)CH_3$) and alcohol ($BrCH(CH_3)CH(CH_3)OH$).

At all temperatures and wavelengths, very good fits of kinetic traces were obtained using an α value that was similar to those measured for the $BrCH_2CH_2O_2$ ($\alpha = 0.57$ at 298 K)[23] and $CH_3CH(CH_3)O_2$ ($\alpha = 0.56$ at 298 K)[3] self-reactions, i.e., $\alpha \approx 0.5$ at 298 K. The systematic uncertainties introduced by this assumption are discussed below.

The averages of optimized values of k_2 are presented as a function of temperature in Table 3. Figure 6 shows the variation of k_2 with temperature in Arrhenius form, yielding the following rate expression:

$$k_2 = (7.60^{+22.05}_{-5.65}) \times 10^{-15} \times \exp\{(1305 \pm 428)\ \mathrm{K}/T\}$$
$$\mathrm{cm^3\ molecule^{-1}\ s^{-1}} \qquad (T = 275{-}371\ \mathrm{K})$$

where the uncertainties represent 95% confidence limits associated with the statistical fitting procedure and include the contribution for the expanded uncertainties in the individual rate constant.

TABLE 4: Rate Constants for Self-Reactions of β-Substituted Ethylperoxy Radicals

radical	k_{298K}[a]	α_{298K}[b]	A[a,c]	E_a/R[d]	ref
$C_2H_5O_2$	8.2×10^{-14}	0.76	6.7×10^{-14}	-60	26
$ClCH_2CH_2O_2$	3.3×10^{-12}	0.63[e]	1.1×10^{-13}	-1020	27
$BrCH_2CH_2O_2$	4.0×10^{-12}[f]	0.57	6.15×10^{-14}	-1247	this work
$HOCH_2CH_2O_2$	2.3×10^{-12}	0.50	6.9×10^{-14}	-1040	10

[a] Given in units of cm^3 molecule^{-1} s^{-1}. [b] Branching ratio for the nonterminating channel. [c] A denotes the pre-exponential factor. [d] Given in kelvin. [e] Arithmetic mean of the value reported by Wallington et al.[28] ($\alpha = 0.69$) and that reported by Yarwood et al.[23] ($\alpha = 0.57$). [f] Recalculated from the Arrhenius expression.

As was done for the previous case, a study of error propagation has been conducted. The formations of HO_2, $BrCH(CH_3)CH(CH_3)OH$, and $BrCH(CH_3)C(O)CH_3$ particularly influence the shape of the experimental traces recorded at wavelengths of <240 nm; therefore, most kinetic measurements were performed at higher wavelengths, where the contributions of the quoted compounds to the total absorption were negligible. Thus, a variation of 30% in the value of α results in a variation of 34% in k_2 at $\lambda = 210$ nm, but a variation of only 10% at $\lambda > 240$ nm. In simulations, the rate constant for the reaction of $BrCH(CH_3)CH(CH_3)O_2$ with HO_2 was estimated to be $k(HOCH(CH_3)CH(CH_3)O_2 + HO_2) = 1.5 \times 10^{-11}$ cm^3 molecule^{-1} s^{-1} at 298 K.[8,9] Reasonably varying this value by a factor of 2 results in a change in the self-reaction rate constant k_2 of 37% at $\lambda = 210$ nm and only 5% at $\lambda = 240$ nm. The total systematic error was finally estimated to be ~23%, yielding an overall propagated error of ~55%.

Discussion and Conclusion

The rate constants of the $BrCH_2CH_2O_2$ and $BrCH(CH_3)CH(CH_3)O_2$ self-reactions have been determined for the first time as a function of temperature. A previous measurement was already reported in the literature by Crowley and Moortgat;[10] however, it was performed at room temperature only, and they only proposed an overall (observed) rate constant of disappearance of the peroxy radicals, without accounting for the complete reaction mechanism. By employing the relation $k_{real} = k_{obs}/(1 + \alpha)$[4] to recalculate the true rate constants k_{real} from the observed rate constant (k_{obs}) data of Crowley and Moortgat,[10] the agreement becomes excellent, despite the discrepancies between the two works observed via UV absorption spectra at short wavelengths. However, this recalculation can be done only when the rate constants for the peroxy self-reaction and its reaction with HO_2 are separated by at least 1 order of magnitude, which is the case for the $BrCH(CH_3)CH(CH_3)O_2$ radical but not that for $BrCH_2CH_2O_2$. In this last case, the complete reaction mechanism must be taken into account to extract k_{real} from experimental data.

A comparison with other rate-constant values for β-monosubstituted ethylperoxy self-reactions is proposed in Table 4. At room temperature, it clearly appears that self-reactions of $C_2H_5O_2$, $ClCH_2CH_2O_2$, $BrCH_2CH_2O_2$, and $HOCH_2CH_2O_2$ all present two channels (see reactions 1a and 1b), with the α values being similar (within uncertainties) for all radicals. In addition, the β-substitution by Cl, Br, or OH results in a large increase in the self-reaction rate constant, by a factor of ~30−50 at 298 K, compared to that of the $C_2H_5O_2$ radical. This may suggest that β-substitution leads to decreased energies of the transition state for decomposition of the stable intermediate of both

TABLE 5: Rate Constants for Self-Reactions of Secondary Peroxy Radicals

radical	k_{298K}[a]	α_{298K}[b]	A[a,c]	E_a/R[d]	ref
$CH_3CH(CH_3)O_2$	1.1×10^{-15}	0.56	1.7×10^{-12}	+2188	4
$BrCH(CH_3)CH(CH_3)O_2$	6.1×10^{-13}[e]	~0.50[f]	7.6×10^{-15}	−1305	this work
$HOCH(CH_3)CH(CH_3)O_2$	6.7×10^{-13}	0.20	7.7×10^{-15}	−1330	9

[a] Given in units of cm^3 $molecule^{-1}$ s^{-1}. [b] Branching ratio for the nonterminating channel. [c] A denotes the pre-exponential factor. [d] Given in kelvin. [e] Recalculated from the Arrhenius expression. [f] See text.

terminating and nonterminating channels in the same way. It may also strengthen the belief that both transition states are identical, as already suggested by Lesclaux.[3] These observations are confirmed when examining the Arrhenius expressions of the self-reaction rate constants in Table 4. The pre-exponential factors are the same (within a factor of <2) and the rate expressions corresponding to $ClCH_2CH_2O_2$, $BrCH_2CH_2O_2$, and $HOCH_2CH_2O_2$ all present a negative temperature coefficient (approximately −1000 K), whereas the $C_2H_5O_2$ self-reaction rate is temperature-independent. Therefore, all the differences observed in the reaction rate constants between unsubstituted and substituted ethylperoxy radicals result more in a change in activation energies (for decomposition of the intermediate complex) than a change in chemical reaction mechanism. The same observations were made, to a lesser extent, for α-substituted methylperoxy radicals.[3]

The self-reaction rate constant of $BrCH(CH_3)CH(CH_3)O_2$ is compared to those of other secondary peroxy radicals in Table 5. It appears that both $BrCH(CH_3)CH(CH_3)O_2$ and $HOCH(CH_3)CH(CH_3)O_2$ present self-reaction rate constants that are a factor of ~600 higher than that of $CH_3CH(CH_3)O_2$, which, until now, has been considered to be a model for the small secondary peroxy radical reactivity.[25] Note the change of the temperature dependence, which becomes negative with the substitution. The rate-constant change from unsubstituted to substituted radicals is not directly a consequence of the temperature dependence; rather, the temperature dependence indicates a drastic change of the reaction mechanism. The presence of a potential barrier indicates a tight transition state and a elementary bimolecular reaction whereas the negative temperature dependence shows the presence of an intermediate potential well and a complex nonelementary reaction mechanism. This also corresponds to very different pre-exponential factors. It should be noted that Arrhenius parameters are remarkably identical for $BrCH(CH_3)CH(CH_3)O_2$ and $HOCH(CH_3)CH(CH_3)O_2$, and that activation energies are also fairly similar to those of primary β-substituted peroxy self-reactions (see Table 4). However, the rate constants for secondary radicals are still a factor of 3−8 smaller than those of their primary homologues. This difference may be explained from pre-exponential factors, which are systematically smaller for secondary substituted peroxy radical reactions.

Similar observations were already reported in previous works by our group on tertiary β-substituted peroxy radicals:[9,11] Tertiary peroxy radical self-reactions present a large activation energy, varying from $E_a/R = 4200$ K for t-$C_4H_9O_2$ to $E_a/R = 1420$ K for the $HOC(CH_3)_2C(CH_3)_2O_2$ radical. No measurement of the variation of the $BrC(CH_3)_2C(CH_3)_2O_2$ self-reaction rate constant, relative to temperature, was possible, because of a change that was occurring in the mechanism at high temperature and was difficult to account for.[11]

We can conclude that substituted peroxy radicals have self-reaction rate constants varying over a much narrower range than unsubstituted radicals, and that the substitution effect does not eliminate the structure effect, even if this latter effect is weakened. Considering the observed structure−activity relationships, it is now possible to make recommendations for self-reaction rate constants of β-substituted peroxy radicals. The recommended values are given in Table 6 for Cl, Br, and OH substituents. Similar trends were observed for multiple fluorine-substituted radicals; however, until now, no data have been available for mono-fluorine-atom substitution. Unfortunately, no data are available for other substituents such as NO_3 and OCH_3. We can probably expect similar enhancements of rate constants compared to unsubstituted radicals.

TABLE 6: Recommended Structure−Activity Relationships for β-Substituted Peroxy Radical Self-Reaction Rate Constants (with Substituent Cl, Br, or OH) as a Function of Temperature

peroxy radical	k_{298K}[a]	uncertainty factor[b]	E_a/R[c]
primary	4×10^{-12}	1.5	−1200
secondary	5×10^{-13}	2	−1200
tertiary	1×10^{-14}	2.5	+1400

[a] Given in units of cm^3 $molecule^{-1}$ s^{-1}. [b] The uncertainty factor is defined as a multiplicative factor reflecting the overall confidence in the rate constant at 298 K, as proposed by the JPL evaluation.[22] [c] Given in kelvin.

Acknowledgment. The authors wish to thank the European Commission for financial support within the Environment and Climate Program.

References and Notes

(1) Atkinson, R.; Baulch, D. L.; Cox, R. A.; Hampson, R. F.; Kerr, J. A.; Rossi, M. J.; Troe, J. *J. Phys. Chem. Ref. Data* **1997**, *26*, 521.

(2) Tyndall, G. S.; Cox, R. A.; Granier, C.; Lesclaux, R.; Moortgat, G. K.; Pilling, M. J.; Ravishankara, A. R.; Wallington, T. J. *J. Geophys. Res.* **2001**, *106* (D11), 12157.

(3) Lesclaux, R. In *Peroxyl Radicals*; Alfassi, Z. B., Ed.; John Wiley: New York, 1997; p 81.

(4) Lightfoot, P. D.; Cox, R. A.; Crowley, J. N.; Destriau, M.; Hayman, G. D.; Jenkin, M. E.; Moortgat, G. K.; Zabel, F. *Atmos. Environ.* **1992**, *26A*, 1805.

(5) Wallington, T. J.; Dagaut, P.; Kurylo, M. J. *Chem. Rev.* **1992**, *92*, 667.

(6) Catoire, V.; Lesclaux, R.; Lightfoot, P. D.; Rayez, M. T. *J. Phys. Chem.* **1994**, *98*, 2889.

(7) Villenave, E.; Lesclaux, R. *Chem. Phys. Lett.* **1995**, *236*, 376.

(8) Jenkin, M. E.; Hayman, G. D. *J. Chem. Soc., Faraday Trans.* **1995**, *91*, 1911.

(9) Boyd, A. A.; Lesclaux, R. *Int. J. Chem. Kinet.* **1997**, *29*, 323.

(10) Crowley, J. N.; Moortgat, G. K. *J. Chem. Soc., Faraday Trans.* **1992**, *88*, 2437.

(11) Villenave, E.; Lesclaux, R. *Int. J. Chem. Kinet.* **2001**, *33*, 41.

(12) Lightfoot, P. D.; Lesclaux, R.; Veyret, B. *J. Phys. Chem.* **1990**, *94*, 700.

(13) Ramacher, B.; Orlando, J. J.; Tyndall, G. S. *Int. J. Chem. Kinet.* **2000**, *33*, 198.

(14) Barnes, I.; Bastian, V.; Becker, K. H.; Overath, R.; Tong, Z. *Int. J. Chem. Kinet.* **1989**, *21*, 499.

(15) Wallington, T. J.; Skewes, L. M.; Siegl, W. O.; Japar, S. M. *Int. J. Chem. Kinet.* **1989**, *21*, 1069.

(16) Knyazev, V. D.; Benczura, A.; Dubinski, I. A.; Gutman, D.; Melius, C. F.; Senkan, S. M. *J. Phys. Chem.* **1995**, *99*, 230.

(17) Lenhardt, T. M.; McDade, C. E.; Bayes, K. D. *J. Phys. Chem.* **1980**, *72*, 304.

(18) Hubinger, S.; Nee, J. B. *J. Photochem. Photobiol. A: Chem.* **1995**, *86*, 1.

(19) Hayman, G. D.; Jenkin, M. E.; Murrels, T. P. *Eurotrac Annual Report, Part 8-Lactoz* **1990**, 113.

(20) Jung, K.-H.; Choi, Y. S.; Yoo, H. S.; Tschuikow-Roux E. *J. Phys. Chem.* **1986**, *90*, 1816.

(21) Hartmann, D.; Karthauser, J.; Sawerysyn, J.-P.; Zellner, R. *Ber. Bunsen-Ges. Phys. Chem.* **1990**, *94*, 639.
(22) DeMore, W. B.; Sander, S. P.; Golden, D. M.; Hampson, R. F.; Kurylo, M. J.; Howard, C. J.; Ravishankara, A. R.; Kolb, C. E.; Molina, M. J. *JPL Publ*. **1997**, *97-4*.
(23) Yarwood, G.; Peng, N.; Niki, H. *Int. J. Chem. Kinet.* **1992**, *24*, 369.
(24) Libuda, H. G.; Shestakov, O.; Theloke, J.; Zabel, F. *Phys. Chem. Chem. Phys.* **2002**, *4*, 2579.
(25) Boyd, A. A.; Villenave, E.; Lesclaux, R. *Int. J. Chem. Kinet.* **1999**, *31*, 37.
(26) Fenter, F. F.; Lightfoot, P. D.; Niiranen, J. T.; Gutman, D. *J. Phys. Chem.* **1993**, *97*, 5313.
(27) Dagaut, P.; Wallington, T. J.; Kurylo, M. J. *Chem. Phys. Lett.* **1988**, *146*, 589.
(28) Wallington, T. J.; Andino, J. M.; Japar, S. M. *Chem. Phys. Lett.* **1990**, *165*, 189.